Calibration of Thermal Models of Steel Continuous Casting Molds

A new methodology is presented to calibrate the 1D CON1D model with a full 3D finite-element model of the mold. The thermocouple depth in the 1D model CON1D is "offset" to account for both the 3D geometric effects and for the heat removed along the thermocouple wire by water or air convection. With the offset, this simple 1D model can match closely with the 3D model. Coupled with models of solidification and interfacial phenomena, this modeling tool is applied to gain insights into many aspects of heat transfer in the process.

The harsh environment of commercial steel continuous casting processes makes taking measurements difficult, expensive and limited with regard to the information gained. Computational models potentially offer deeper knowledge, but only if they can accurately predict the plant behavior. This requires including and solving the equations which govern all of the important physical phenomena. To achieve reasonable speed while retaining accuracy, computational models must be simplified and calibrated to match plant experiments, using parameters which remain constant over the range of processing conditions of interest. Only after verification, calibration and validation can a model be used reliably as a predictive tool to investigative complex processes such as continuous casting.

Development of an accurate computational model requires verification, calibration and validation. Verification refers to matching the model predictions exactly with the known analytical solution of a simple, well-defined test problem, in order to prove error-free programming of the chosen numerical methods, and to find reasonable choices for mesh and time-step discretizations. Validation refers to matching the model predictions with plant experiments to ensure that the equations being solved contain the appropriate physics, and that the properties and constants in those equations have good values. Calibration is usually needed to find values for those constants to match the plant measurements and achieve validation. These last two activities generally require multiple iterations. This paper illustrates this activity for the computational model of heat transfer in continuous casting of steel, CON1D.[1]

The CON1D model has been successfully applied to many commercial casters in previous work,[2–6] and is described in detail elsewhere.[1] This paper focuses on the calibration procedure to improve its accuracy. The procedure first involves a full 3D computation of the mold to produce average results for a "calibration domain." Input parameters to the CON1D model are defined and calibrated to match the average hot face and thermocouple temperatures from the 3D model. Then, CON1D can be calibrated to match thermocouple measurements and heat flux measurements taken from plant operation. Finally, the model can be applied to gain new insights into the process.

Authors

Lance C. Hibbeler (left) (lhibbel2@illinois.edu), Melody M. Langeneckert, Junya Iwasaki, Inwho Hwang (hwang104@illinois.edu), and Brian G. Thomas (center), professor, Department of Mechanical Science and Engineering (bgthomas@illinois.edu), University of Illinois at Urbana-Champaign, Department of Mechanical Science and Engineering, Urbana, Ill., USA; and Ron J. O'Malley (right), plant metallurgist (ron.omalley@nucor.com), Nucor Steel–Decatur LLC, Trinity, Ala., USA

3D Model of Mold: Calibration Domain

The steady-state temperature distribution in the continuous casting mold is determined by solving the steady heat-conduction equation for temperature as a function of the three coordinate directions, $T(x,y,z)$:

$$\frac{\partial}{\partial x}\left(k\frac{\partial T}{\partial x}\right)+\frac{\partial}{\partial y}\left(k\frac{\partial T}{\partial y}\right)+\frac{\partial}{\partial z}\left(k\frac{\partial T}{\partial z}\right)=0 \qquad \text{(Eq. 1)}$$

where

k is the isotropic thermal conductivity.

The temperature dependence of the thermal conductivity of mold copper alloys of about –0.05%/°C has only a small effect on the typical mold temperature field.[7] This effect is readily included, but the governing equation for the calibration procedure is simplified here for constant conductivity:

$$\frac{\partial^2 T}{\partial x^2}+\frac{\partial^2 T}{\partial y^2}+\frac{\partial^2 T}{\partial z^2}=0 \qquad \text{(Eq. 2)}$$

Boundary conditions include specified heat flux at the mold hot face:

$$-k_0\frac{\partial T}{\partial n}=q_0 \qquad \text{(Eq. 3)}$$

where

k_0 is the average thermal conductivity,
q_0 is the heat load that may vary with position and
$\partial T/\partial n$ is the temperature gradient normal to the mold surface.

On the water channels, a constant convection condition is specified:

$$-k_0\frac{\partial T}{\partial n}=h_0\left(T-T_0\right) \qquad \text{(Eq. 4)}$$

by defining the heat transfer coefficient and "sink" temperature, T_0.

The finite element method is used to solve these equations in the complicated-shaped domain of the modern casting mold, owing to its accurate handling of arbitrary geometries. This work uses the commercial finite-element software ABAQUS,[9] combined with scripts written in Python code to automate creation of the geometry, running of the analysis and post-processing the results to extract the parameters needed for the 1D CON1D model, as discussed later. The aim of this model is to enable the simple 1D model of the mold, CON1D, to achieve the accuracy of a complete 3D analysis of the multidimensional heat flow around the roots of water channels and thermocouple holes.

The 3D model domain should reproduce the exact geometry of an appropriate periodic or symmetric portion of the mold geometry. The 3D model results can be used directly to reveal local heat transfer variations within this fundamental domain, such as hot face temperature variations around the mold perimeter between bolts. For the calibration of the 1D model, the 3D model results are spatially averaged over this symmetrically repeating domain, to extract the average hot face temperature $T_{hot,3D}$, the average cold face temperature $T_{cold,3D}$, and the average temperature on the small surface that contacts the thermocouple $T_{TC,3D}$. These three temperatures are needed for the 1D model calibration. In addition, the 3D model results reveal insights into important mold temperature variations. Modern computer platforms can solve this problem, even with very fine mesh resolution, with execution times on the order of a few minutes.

1D Model of Mold

Modeling heat transfer in continuous casting requires accurate incorporation of the mold, interface and solidifying shell. Away from the corners, many phenomena can be modeled reasonably well with a 1D assumption. The CON1D model is based on a 1D finite-difference solidification model of the shell, taking advantage of the large Péclet number that makes axial heat conduction negligible relative to heat transported by the moving steel. It includes conduction and radiation across the interfacial layers, aided by mass, momentum and force balances on the slag, which are all solved analytically. For efficiency, heat conduction through the mold is modeled analytically. Axial heat conduction in the mold, which is important near the meniscus, is handled with a two-dimensional series solution.[1,2,4] Through the thickness direction, the coated copper plate is treated as a series of 1D thermal resistances. The water slot region is treated as a convection surface in parallel with heat-conduction fins. Further details are given as follows.

The mold in the CON1D model is envisioned as a rectangular block with rectangular water channels, as shown in Figure 1. All water channels are identical

with depth, d_c; width, w_c; and pitch, p_c. The hot side of the mold is supplied a heat flux, q_{hot}, from the interface and solidification models, described elsewhere.[1] Heat is extracted from the water channel surfaces via a convection condition, $h_{cold}(T_{cold}–T_{water})$. The temperature distribution inside the mold is found by integrating directly Equation 1 and applying these two boundary conditions:

$$T(x) = T_{water} + q_{hot}\left(\frac{1}{h_{cold}} + \frac{d_{mold} - x}{k_{mold}}\right)$$

(Eq. 5)

where

x is the distance away from the hot face and
d_{mold} is the simulated mold thickness.

Coating layers are included by adding $d_{coating}/k_{coating}$ resistors inside the parentheses.[1] This gives a cold face temperature of $T_{cold} = T(d_{mold}) = T_{water} + q_{hot}/h_{cold}$ and a hot face temperature of $T_{hot} = T(0) = T_{water} + q_{hot}(1/h_{cold} + d_{mold}/h_{cold})$. The cold side heat transfer coefficient is adjusted to include scale deposits as another thermal resistance:

$$\frac{1}{h_{cold}} = \frac{d_{scale}}{k_{scale}} + \frac{1}{h_w}$$

(Eq. 6)

where

d_{scale} and k_{scale} are the thickness and thermal conductivity of any scale layers on the channel sides and
h_w is the fin-enhanced heat transfer coefficient of the nominal water convection coefficient h_{water}:

$$h_w = h_{water}\frac{w_c}{p_c} + \frac{1}{p_c}\sqrt{2(p_c - w_c)h_{water}k_{mold}}\tanh\left(d_c\sqrt{\frac{2}{(p_c - w_c)}\frac{h_{water}}{k_{mold}}}\right)$$

(Eq. 7)

The first term on the right-hand side accounts for the heat leaving the roots of the channels, while the second term accounts for the heat transferred through the lateral surfaces of the fins. This equation assumes a large number of rectangular channels that are very long in the casting direction, and that heat loss into the backing plate or waterbox is negligible. Of many empirical correlations for the water convection coefficient, the forced-internal-flow correlation of Sleicher and Rouse[10] is chosen for its accurate fit with many measurements (about 7% average error):

Figure 1

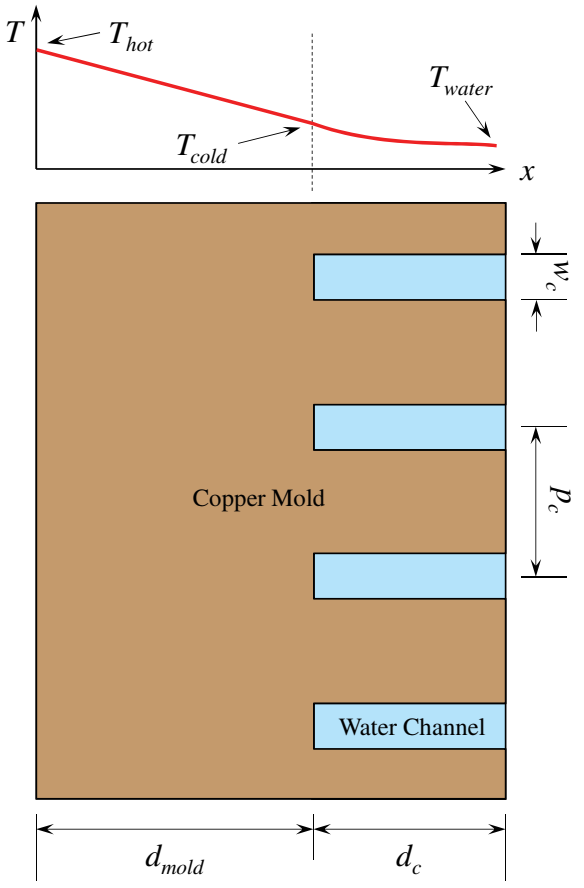

1D mold model.

$$\mathrm{Nu} = 5 + 0.015\,\mathrm{Re}^a\,\mathrm{Pr}^b$$

(Eq. 8)

The Nusselt number, $\mathrm{Nu} = h_{water}D_h/k_{water}$; Prandtl number, $\mathrm{Pr} = \mu_{water}c_{p,water}/k_{water}$; and Reynolds number, $\mathrm{Re} = \rho_{water}V_{water}D_h/\mu_{water}$ are evaluated, respectively, at the temperature of the bulk water, T_{water}; the temperature of the channel surface, T_{cold}; and the "film" temperature, $T_{film} = \frac{1}{2}(T_{water} + T_{cold})$. The hydraulic diameter, defined as four times the cross-sectional area divided by the perimeter, is $D_h = 2w_cd_c/(w_c + d_c)$ for a rectangular channel, and $a = 0.88–0.24/(4 + \mathrm{Pr})$ and $b = 1/3 + 0.5\exp(–0.6\ \mathrm{Pr})$ are fitting constants. The water velocity, V_{water}, is found from the total water flowrate in the plant and the total water channel area. The water properties[4] vary with temperature (°C) as follows:

$$k_{water}(T) = 0.59 + 0.001 \cdot T$$

(Eq. 9)

$$\mu_{water}(T) = 2.062 \cdot 10^{-9} \rho_{water} \cdot 10^{792.42/(T+273.15)}$$

(Eq. 10)

$$\rho_{water}(T) = 1000.3 - 0.040286 \cdot T - 0.0039779 \cdot T^2$$

(Eq. 11)

$$c_{p,water}(T) = 4215.0 - 1.5594 \cdot T + 0.015234 \cdot T^2$$

(Eq. 12)

Measurements available at most casters include thermocouple temperatures and the average heat flux, based on the mold water flowrate and its temperature increase. In the 1D CON1D model approximation, thermocouple temperatures, T_{TC}, are obtained by evaluating Equation 5 at the appropriate distance beneath the hot face, d_{TC}:

$$T_{TC} = T_{water} + q_{hot}\left(\frac{1}{h_{cold}} + \frac{d_{mold} - d_{TC}}{k_{mold}}\right)$$

(Eq. 13)

The increase in temperature of the mold water as it flows through the channels is found by applying a heat balance on a differential slice through the water and integrating over the working mold length:

$$\Delta T_{water}(z) = \frac{p_c}{w_c d_c} \frac{1}{V_{water}} \int_0^z \frac{q_{hot}(z')}{\rho_{water}(z') c_{p,water}(z')} dz'$$

(Eq. 14)

where

z is the distance below the meniscus.

This assumes that all heat entering the mold is removed by the mold water. This prediction of mold temperature rise must be modified to account for unused water channels when casting narrow slabs relative to the mold width and, if applicable, the fact that the water channels might not all have the same dimensions and pitch:

$$\Delta T'_{water} = \Delta T_{water} \frac{w_{slab}}{p_c} \frac{w_c d_c}{A_{channels}}$$

(Eq. 15)

where

w_{slab} is the slab width and
$A_{channels}$ is the total cross-sectional area of the channels.

After geometric calibration described in the next section, a second calibration/verification stage should be performed to ensure that this prediction of the water temperature rise matches with the plant measurements.

1D Model Calibration

Simplifying the mold geometry for the 1D model requires careful definition of the dimensions in order to retain the thermal characteristics of the system. The geometric parameters in the 1D model described above are the simulated mold thickness, d_{mold}; the channel width, w_c; the channel depth, d_c; and the channel pitch, p_c. By choosing these parameters carefully, the 1D model can attain the predictive capability of the 3D finite-element calculation mentioned previously. This section presents the equations to accomplish this, which have been implemented into the Python script and are executed after post-processing of the finite-element results, prior to running CON1D.

Water Channel Geometry — The water channels in the 1D model must have identical cross-sectional area to the physical mold to maintain the mass flowrate of the cooling water. To maintain the convection coefficient in the water channels, the hydraulic diameter must be the same as well. For a single channel, this requires:

$$w_c d_c = A_{c,actual}$$

(Eq. 16a)

$$\frac{2 w_c d_c}{(w_c + d_c)} = D_{h,actual}$$

(Eq. 16b)

where

$A_{c,actual}$ and $D_{h,actual}$ are the cross-sectional area and hydraulic diameter of the actual channel.

These two equations are solved simultaneously to give:

$$w_c, d_c = A_{c,actual}/D_{h,actual} \pm \sqrt{\left(A_{c,actual}/D_{h,actual}\right)^2 - A_{c,actual}}$$

(Eq. 17)

where the smaller of the two roots is the channel width and the larger root is the channel depth. Note that both roots are positive because $A_{c,actual}$ and $D_{h,actual}$ are positive. If the mold has different types of channels, which is common around bolt holes, then the actual channel area and hydraulic diameter should be their respective averages for all N channels across the width of the repeating portion of the mold, modeled in the 3D calculation:

$$A_{c,actual} = \frac{1}{N}\sum_{i=1}^{N} A_{c,actual,i}$$

(Eq. 18a)

$$D_{h,actual} = \frac{1}{N}\sum_{i=1}^{N} D_{h,actual,i}$$

(Eq. 18b)

Note that Equation 17 is not applicable if all channels are round. An approximation that relaxes Equation 16b is used for this case.[6] Specifically, setting w_c = 0.7 D produces an error in the convection coefficient of only 2%.

The simulated channel pitch should be chosen to minimize the variations caused by different channel sizes. Consider the cumulative channel cross-sectional area plotted with distance along a symmetric portion of the mold width, schematically illustrated in Figure 2. The 1D model approximates this cumulative area as a straight line with a slope that defines the simulated channel pitch, p_c:

$$A_{cumulative,simulated}(x) = \frac{A_{c,actual}}{p_c}x$$

(Eq. 19)

The details of the actual cumulative area function are specific to an individual mold, but a simple least-squares fit is sufficient to determine a good simulated pitch.

Next, the simulated mold thickness, d_{mold}, should be chosen such that the hot face temperature matches the 3D simulation under identical boundary conditions. Evaluating Equation 5 at the hot face, matching the result to the average hot face temperature calculated with the 3D model, and rearranging, gives:

Figure 2

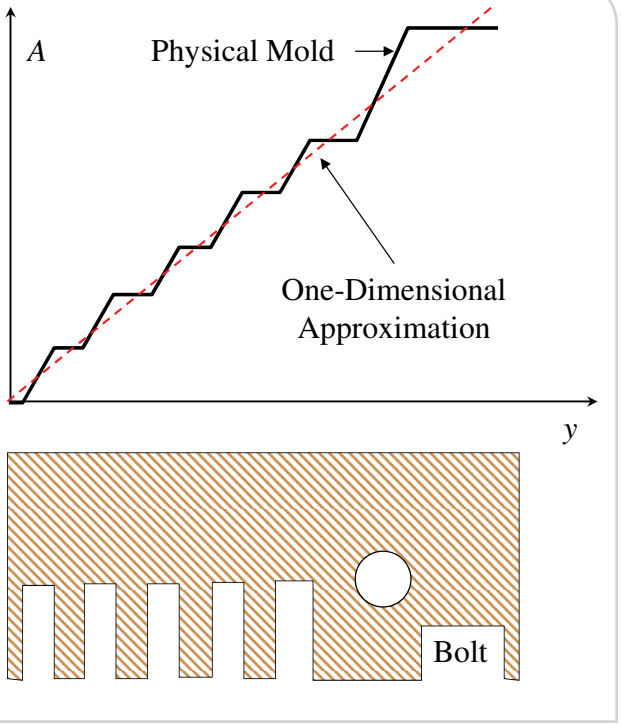

Simulated channel pitch should match cumulative channel area.

$$d_{mold} = \frac{k_0}{q_0}\left(T_{hot,3D} - T_{w0}\right) - \frac{k_0}{h_{cold}}$$

(Eq. 20)

Since $h_{cold} >> k_{mold}$, the second term of Equation 20 usually is negligible. To match the 3D calculation, the temperature dependency of the properties and the scale layer are neglected during calibration, so Equations 6 and 7 simplify to:

$$h_{cold} = h_0\frac{w_c}{p_c} + \frac{1}{p_c}\sqrt{2\left(p_c - w_c\right)h_0 k_0}\tanh\left(d_c\sqrt{\frac{2}{\left(p_c - w_c\right)}\frac{h_0}{k_0}}\right)$$

(Eq. 21)

Note that for some geometries, this calibration method causes the parameter d_{mold} to be significantly larger than the distance between the hot face and water channel roots, d_{cold}. The distance from the hot face to where the cold face temperature is found in the 1D model is defined as:

$$d'_{mold} = d_{mold} - \frac{k_0}{q_0}\left(T_{cold,3D} - T_{w0}\right) = \frac{k_0}{q_0}\left(T_{hot,3D} - T_{cold,3D}\right)$$

(Eq. 22)

Depending on the choice of $T_{cold,3D}$, the cold face temperature predicted by CON1D can be chosen to match the root, average or other desired definition of cold face temperature. Defining the cold face temperature as the average root temperature over all channels gives d'_{cold} close to the physical distance between the hot face and water channels.

This calibration method enables the 1D model to match the hot face and cold face temperatures calculated in the 3D model by changing the water channel input geometry in a physically based manner.

Thermocouple Hole Geometry — The thermocouple temperature predicted by the CON1D model may differ from the temperature predicted by the 3D finite-element model at the same location.[6,11] Depending on the geometry, this error has been observed to exceed 50 °C. This mismatch is due to the inability of the 1D model to capture the effects of complicated geometry near the thermocouple bore. However, this problem can be overcome by changing the location of the simulated thermocouple. By moving the thermocouple point in the 1D model closer to the hot face, the 1D model can reliably reproduce the hotter thermocouple temperature predicted by the 3D model, regardless of heat flux, mold material and water channel behavior.

By manipulating Equation 13, the simulated thermocouple depth in the calibrated 1D model should be:

$$d'_{TC} = d_{mold} - \frac{k_0}{q_0}\left(T_{TC,3D} - T_{w0}\right) = \frac{k_0}{q_0}\left(T_{hot,3D} - T_{TC,3D}\right) \quad \text{(Eq. 23)}$$

This calibration of the thermocouple location should be performed after the water channel geometry has been calibrated using Equations 17, 19 and 21. Even though the terms appear in Equation 23, d'_{TC} is independent of heat flux, conductivity and mold geometry. This observation is demonstrated later.

Offset Methodology — In the interest of a user-friendly model interface, it is convenient to express each calibrated dimension as the "blueprint" value and an "offset" distance. This approach also illustrates the importance of the calibrations. For example, the mold thickness offset distance, Δd_{cold}, is defined as:

$$\Delta d_{cold} = d'_{cold} - d_{cold} \quad \text{(Eq. 24)}$$

and the thermocouple offset distance, Δd_{TC}, is:

$$\Delta d_{TC} = d'_{TC} - d_{TC} \quad \text{(Eq. 25)}$$

Because calibration is independent of heat load and mold properties, the offset calculation needs to be performed only once for a given mold geometry.

Thermocouple Wire Heat Removal — Measured thermocouple temperatures often read low due to contact resistance between the thermocouple bead and the cold face where the thermocouple is touching. Heat is lost by conduction along the length of the thermocouple wires, especially if they are long and well cooled. Assuming that the thermocouples behave as long, circular rod-fins, they extract heat with a rate of:

$$q_{TC} = \sqrt{\frac{4}{D} h\, k_{TC}}\ \left(T_{TC} - T_0\right) \quad \text{(Eq. 26)}$$

where

D is the thermocouple diameter,
k_{TC} is the conductivity of the thermocouple,
h is the heat transfer coefficient along the thermocouple wire to the surrounding medium at temperature T_0, and
T_{TC} is the thermocouple temperature.

The heat transfer coefficient should be around 5 kW/m²·K for water or 0.1 kW/m²·K for air.

The thermocouple temperature, T'_{TC}, accounting for this heat loss, can be modeled using another heat-conduction resistor:

$$T'_{TC} = T_{TC} + \frac{d_{gap}}{k_{gap}} q_{TC} \quad \text{(Eq. 27)}$$

where

T_{TC} is the predicted thermocouple temperature which, for the 1D model, is from Equation 13, using the calibrated thermocouple depth, d'_{TC}, from Equation 22 and
d_{gap} and k_{gap} are the size and thermal conductivity of the gap between the thermocouple and the mold copper.

The gap conductivity should be about 1.25 W/m·K for a thermal paste, or about 0.04 W/m·K for dry, still air. The gap size is typically on the order of 0.01–0.1 mm, but can be treated as a calibration parameter to force the models to match plant measurements. This approach of calibrating thermocouple temperatures has been demonstrated in recent works presented elsewhere.[12,13]

Example Calibrations

The calibration procedure presented in this work is demonstrated for two commercial casting molds with complicated mold geometries. Both are uncoated thin-slab mold wide faces, one with and one without a funnel. Four cases, summarized in Table 1, are considered to prove the method for different geometries and processing conditions.

Mold A is 1,986 mm wide, 950 mm long and 40 mm thick. It has a rectangular array of mold bolts at 108 mm in the width direction and 133 mm in the casting direction, except for the top and bottom row of bolts. There are three rows of thermocouples at 205 mm, 355 mm and 505 mm below the top of the mold, spaced at 108 mm in the width direction, directly between bolt columns. The calibration domain models a typical thermocouple in the middle row of thermocouples, extending to its four nearest bolts. The periodic nature of this mold geometry allows use of the "fundamental" calibration domain, shown in Figures 3–5. As seen in Figure 3, the water channels immediately adjacent to the bolt columns curve around the bolt holes; except for these regions, the channel pitch is 17.7 mm. Each fundamental domain has six 16-mm-deep ball-end-milled channels, which run almost the entire length of the mold between any two adjacent columns of bolt holes. The two channels directly adjacent to a column of bolt holes are 6 mm wide, while the "standard" channels are 5 mm wide.

Mold B is 1,860 mm wide, 1,100 mm long and 80 mm thick. It has a funnel that is 750 mm wide with a 260-mm-wide "inner flat" region. The funnel tapers from a 23.4-mm crown to an 8-mm crown at mold exit. This mold has a rectangular array of mold bolts at 212.5 mm in the width direction and 125 mm in the casting direction. There is a thermocouple hole drilled into every bolt hole, except for the topmost row and outermost columns of bolts. The water channels consist of banks of 18 ball-end-milled channels, 5 mm across, 15 mm deep and 10 mm pitch, between two bolt columns, with gun-drilled 12-mm circular channels immediately adjacent to the bolt holes. The calibration domain models a typical thermocouple outside of the funnel region, and includes one circular channel and nine ball-end-milled channels.

3D Model Results — The 3D model of the mold contains the exact geometry of a portion of the mold geometry, chosen here as the fundamental domain shown in Figure 3, for case 1. The three process parameters input to this model are simply:

Table 1

Simulation Parameters and Results

	Case 1		Case 2		Case 3		Case 4	
Mold	A 3D	A 1D	A 3D	A 1D	B 3D	B 1D	B 3D	B 1D
Thermal conductivity k_0 (W/m·K)	340		326		350		300	
Heat flux q_0 (MW/m²)	2.10		2.35		3.00		2.71	
Water HTC h_0 (kW/m²·K)	32.5		29.0		40.0		27.0	
Water temperature T_{w0} (°C)	31.0		30.0		35.0		37.0	
Hot face temperature T_{hot} (°C)	248	248.1	286	287.1	312	310.4	339	340.3
Mold thickness d_{mold} (mm)	36.0	35.1	36.0	35.5	35.0	32.3	35.0	33.4
Cold face temperature T_{cold} (°C)	96.6	96.6	107	106.8	97.4	97.2	114.3	115.5
Distance to cold face d_{cold} (mm)	24	24.6	24	24.9	25	25.0	25	24.9
Cold face offset Δd_{cold} (mm)	—	–0.61	—	–0.90	—	–0.04	—	0.13
Thermocouple temperature T_{TC} (°C)	146.0	146.3	167.0	168.3	159.7	159.8	180.3	181.5
Distance to thermocouple d_{TC} (mm)	18	16.51	18	16.51	20	17.77	20	17.57
Thermocouple offset Δd_{TC} (mm)	—	1.49	—	1.49	—	2.23	—	2.43

Figure 3

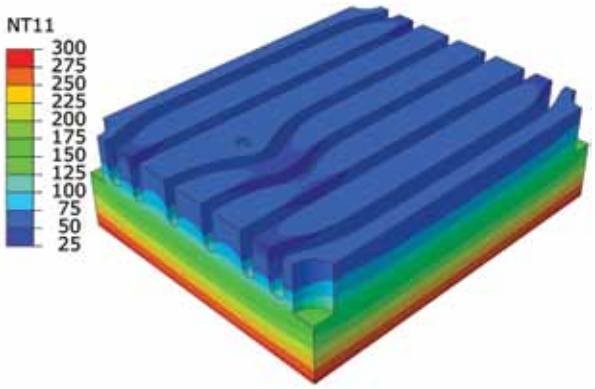

Mold temperatures (°C) in mold calibration domain from 3D model (case 1).

Figure 4

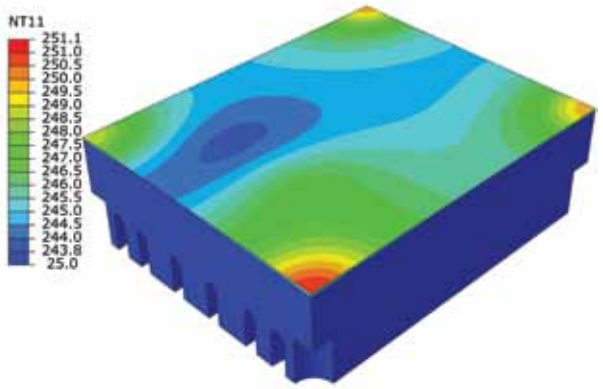

Hot face temperatures (°C) in mold calibration domain from 3D model (case 1).

Figure 5

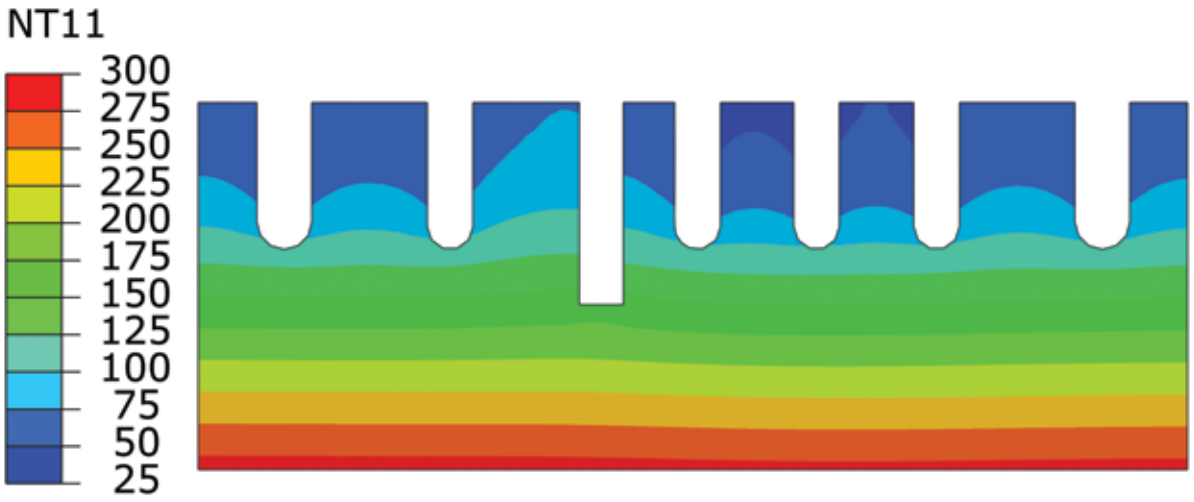

Mold temperatures (°C) from 3D model near thermocouple (case 1).

- The mold conductivity, k_0.
- A uniform heat flux to the hot face, q_0.
- A uniform water channel convection coefficient, h_0, and water temperature, T_{w0}.

The finite element model predicts hot face temperatures ranging from 243.8 to 251.1 °C with an average hot face temperature $T_{hot,3D}$ = 248 °C, average cold face temperature $T_{cold,3D}$ = 96.6 °C, (taken at the water channel roots), and thermocouple temperature $T_{TC,\ 3D}$ = 146 °C. The calculated temperature contours for case 1 are shown in Figures 3–5. These results show that the highest hot face temperature in this mold geometry, found opposite the bolt nearest to the thermocouple, is about 7 °C hotter than the minimum temperature around the mold perimeter. It is not known if this hot face temperature variation is significant for longitudinal crack formation.

Geometric Calibration of CON1D With 3D Model

— Equation 17 gives the calibrated channel width and depth as 5.647 mm and 14.566 mm, respectively. Figure 6 shows the determination of the channel pitch as 18.05 mm (average channel area of 82.26 mm² divided by the least-squares slope of 4.556 mm²/mm). Using Equation 21, the effective heat transfer coefficient is then 37.65 kW/m²·K, so Equation 20 gives the calibrated mold thickness as 35.12 mm. Using

Figure 6

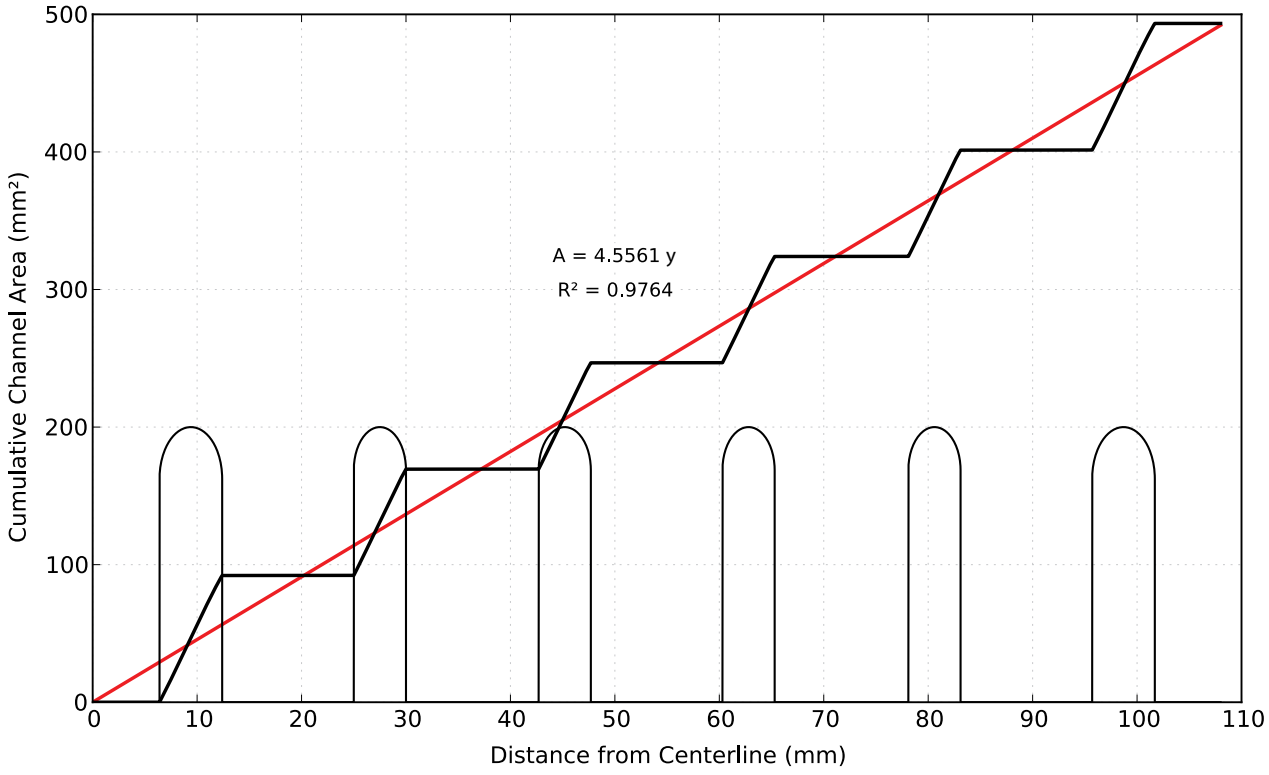

Determination of the 1D channel pitch.

identical boundary conditions and these calibrated geometries in CON1D gives a hot face temperature of 248.1 °C, which matches well with the 3D model. Using a thermocouple depth of 16.52 mm as calculated by Equation 23 instead of the nominal 18 mm (offset of 1.48 mm), the CON1D thermocouple temperature is 146.27 °C, which again matches well with the 3D model. Using a cold face depth of 24.61 mm instead of the nominal 24 mm (offset of 0.61 mm), the CON1D prediction exactly matches the 3D model cold face temperature of 96.6 °C.

Table 1 shows the results of implementing this calibration procedure for different geometries and different processing parameters. Repeating the calibration procedure after changing the boundary conditions and thermal conductivity for mold A (case 2) gives very similar calibrated geometries. For mold B, the calibrated channel is 5.84 mm wide and 13.07 mm deep, with a pitch of 10.63 mm. Again, repeating the calibration procedure with different thermal loading conditions and material properties, produces nearly identical calibrated distances for the same mold geometry. The thermocouple offsets of 2.23 and 2.43 mm reported here are nearly the same as the 2.41 mm offset that was calculated in previous work.[6] More careful calculation of the average temperatures would likely produce calibrated distances that are even more similar. Nevertheless, the calibration procedure outlined here is independent of boundary conditions, and only needs to be performed once per mold geometry.

Heat Transfer Calibration of CON1D With Plant Data — Once the mold geometry has been properly calibrated, the mold water heat removal predicted by CON1D should be calibrated to match plant measurements. Previous work[6] details this process for a wide variety of conditions for mold B. For example, consider casting a 0.045%C steel at 4.5 m/minute: the plant measures 2.55 MW/m² and CON1D calculates 2.54 MW/m² after calibration. Figure 7 shows that the CON1D predictions of thermocouple temperatures, once calibrated for geometric effects, match well with the maximum of the plant measurements at all thermocouples. The thermocouple calibration procedure was performed only once in this case, assuming perfect contact ($d_{gap} = 0$), and was applied to all thermocouples in the simulated mold. Intermittent nonzero contact resistance is believed to explain why some of the plant thermocouples give lower temperatures.

Figure 7

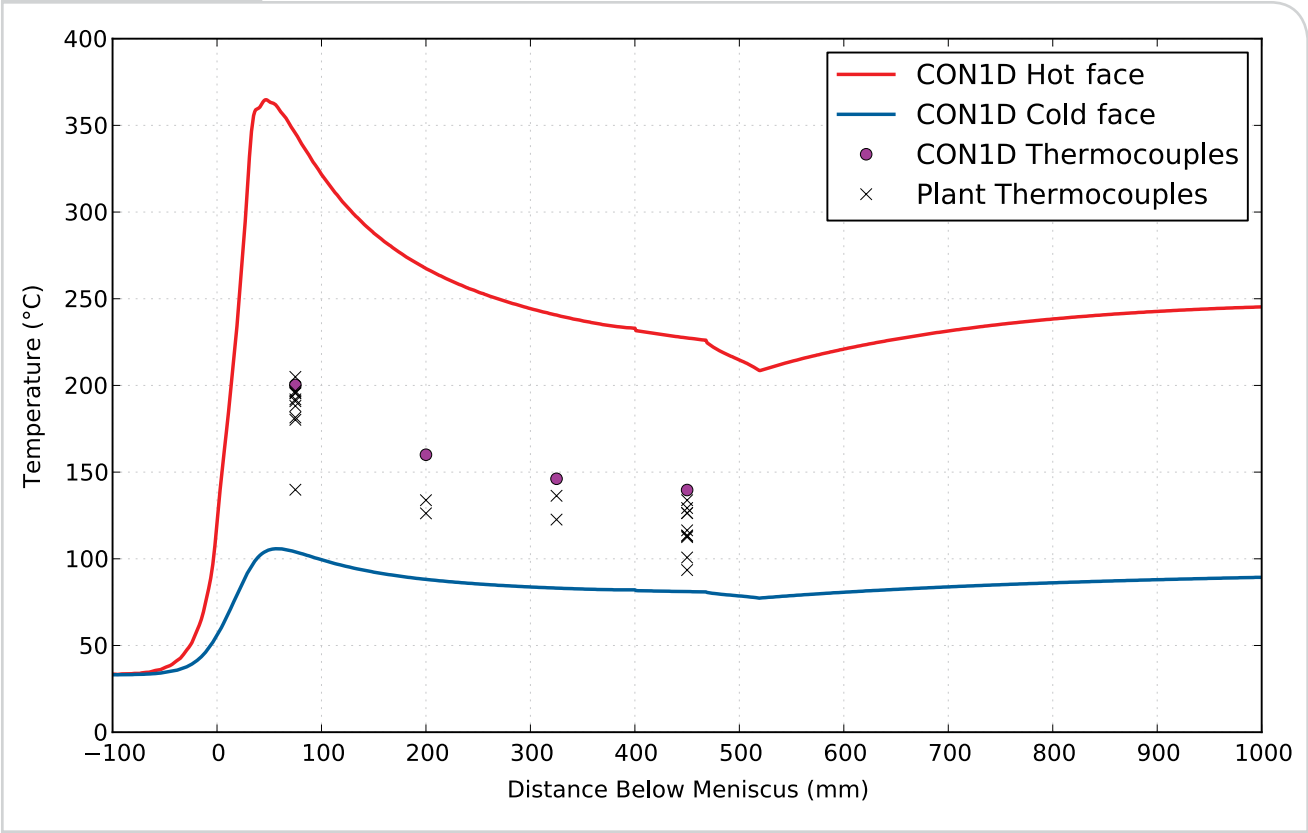

Calibrated CON1D matches plant thermocouple measurements.[6]

Example Application: Effect of Mold Wear on Scale Formation

After it has been calibrated both geometrically with the 3D model and thermally with plant measurements, as described in the previous section, the accurate 1D model is ready to apply to investigate a variety of heat transfer phenomena. As a simple example application, the CON1D model that was calibrated and validated in this work for mold A was applied to study the formation of scale as the mold wears. Scale is assumed to form when the water in the channels is first able to boil, which is assumed to be a possibility when the surface temperature of the root of the channel — the calibrated cold face temperature — exceeds the boiling temperature. The boiling temperature in °C depends on the pressure as follows:[14]

$$T_{boil} = \frac{1810.94}{8.14019 - \log_{10}(7500.62 \cdot p)} - 244.485 \quad \text{(Eq. 28)}$$

where

p is the local pressure in the cooling channels in MPa.

As the distance to the channels decreases with mold wear, the mold hot face temperature decreases, but the cold face temperature increases, for a given heat flux. Using Equation 28 with the CON1D results, the critical peak heat flux into the mold at which boiling and scale deposits could form can be identified. At the example operation pressure of 1.1 MPa, the critical cold face temperature is 184.3 °C, and the critical local heat flux drops from 5.15 to 3.68 MW/m^2 with just 4 mm of mold wear. Scale layers serve to increase mold temperature: specifically, CON1D predicts that a 5-µm-thick scale layer will increase both hot face and cold face surface temperatures by more than 20 °C. Some worn molds have been observed to operate with higher average heat removal, and the smaller resistance to heat flow from the thinner mold is insufficient to explain this.[6] The application here suggests that scale formation associated with the mold wear could be a possible explanation.

Figure 8

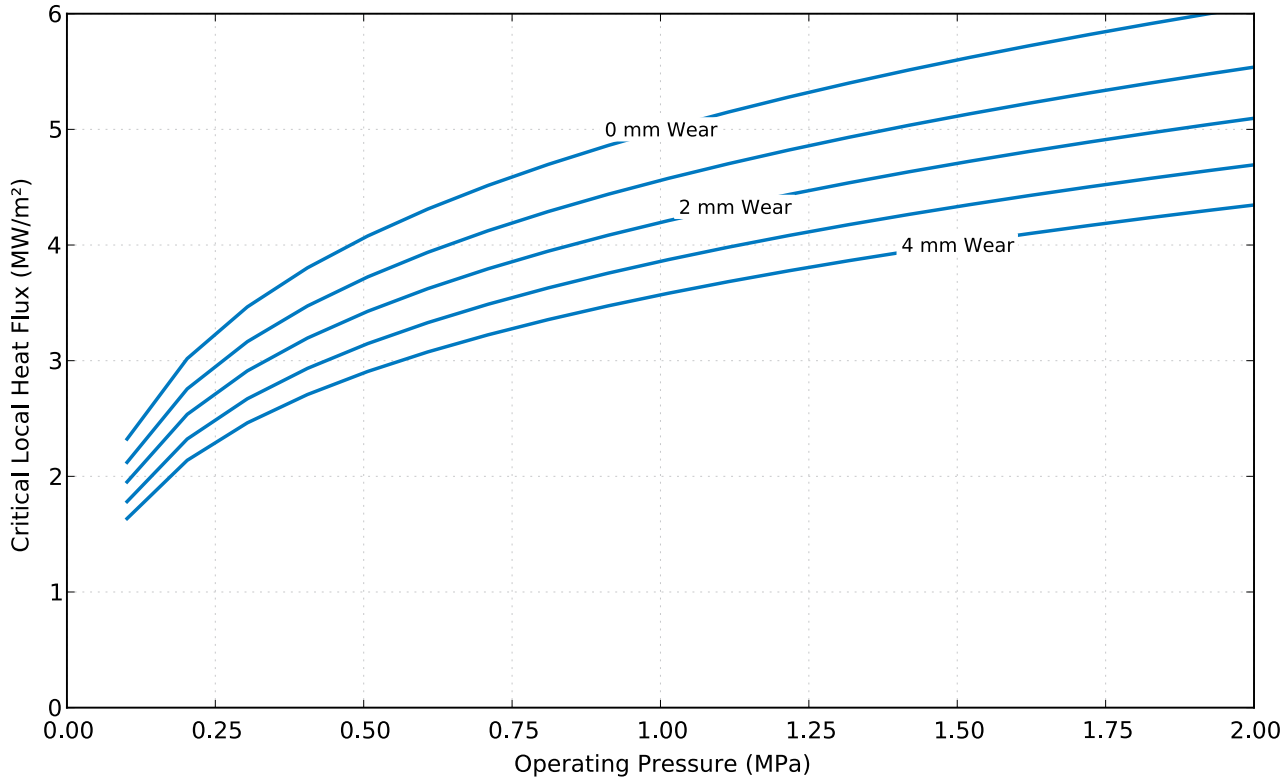

Critical heat flux for scale formation decreases as mold wear increases.

Scale formation problems can be minimized by maintaining high-purity water quality, keeping high water velocity, and careful design of water channels and water delivery system to avoid pressure drops. Note also that thinner molds tend to have lower temperatures, which helps to prevent scale formation with a lower cold face temperature. However, since the heat transfer from the shell into the mold depends on the interfacial gap resistance associated more with hot face temperature, the net effect on overall heat transfer depends on the mold flux behavior.[6] The results here suggest that molds should be paired as matching sets, wear should be regularly monitored and water channels should be carefully inspected for scale formation.

Conclusions

This work has derived and demonstrated a method for imparting the accuracy of a 3D mathematical model of mold heat transfer into a 1D model of the continuous casting process. Specifically, the water channel geometries and thermocouple position are changed slightly from their respective "blueprint" values to compensate for multidimensional heat transfer. The calibration procedure was demonstrated to be independent of process conditions, so it needs to be performed only once per mold geometry. Once this geometric calibration is performed, the shell-mold interfacial parameters in the fast 1D model can be calibrated to match plant data, and then the model can be applied to accurately investigate various aspects of heat transfer in the continuous casting process.

An example application is provided to show that a scale layer is more likely to form for older, thinner molds. The 3D models used in this work show the variation of mold surface temperature due to the geometric features of the mold. Future work is needed to quantify the allowable variability in mold surface temperature to avoid defects in the cast steel.

Acknowledgments

The authors gratefully acknowledge the financial support of the member companies of the Continuous Casting Consortium at the University of Illinois at Urbana-Champaign, and the National Science Foundation (Grant CMMI 09-00138 REU).

References

1. Y. Meng and B.G. Thomas, "Heat Transfer and Solidification Model of Continuous Slab Casting: CON1D," *Metallurgical and Materials Transactions,* Vol. 34B, No. 5, 2003, pp. 685–705.
2. M.R. Ridolfi, B.G. Thomas, G. Li and U. Della Foglia, "The Optimization of Mold Taper for the Ilva-Dalmine Round Bloom Caster," *La Revue de Metallurgie — CIT,* Vol. 91, No. 2, 1994, pp. 609–620.
3. J. Sengupta, M.K. Trinh, D. Currey and B.G. Thomas, "Utilization of CON1D at ArcelorMittal Dofasco's No. 2 Continuous Caster for Crater End Determination," *AISTech Conference Proceedings,* Vol. II, 2009, pp. 1125–1133.
4. G. Li, B.G. Thomas, B. Ho, G. Li and N. Youssef, "CON1D User Manual," *CCC Report,* University of Illinois, July 1992.
5. Y. Meng and B.G. Thomas, "Simulation of Microstructure and Behavior of Interfacial Mold Slag Layers in Continuous Casting of Steel," *ISIJ International,* Vol. 46, No. 5, 2006, pp. 660–669.
6. B. Santillana, L.C. Hibbeler, B.G. Thomas, A. Hamoen, A. Kamperman and W. van der Knoop, "Heat Transfer in Funnel Mold Casting: Effect of Plate Thickness," *ISIJ International,* Vol. 48, No. 10, 2008, pp. 1380–1388.
7. I.V. Samarasekera and J.K. Brimacombe, "The Thermal Field in Continuous-Casting Molds," *Canadian Metallurgical Quarterly,* Vol. 18, No. 3, 1979, pp. 251–266.
8. S. Chenna Krishna, N. Supriya, Abhay K. Jha, Bhanu Pant, S.C. Sharma and Koshy M. George, "Thermal Conductivity of Cu-Cr-Zr-Ti Alloy in the Temperature Range of 300–873 K," *ISRN Metallurgy,* Vol. 2012, Article ID 580659, 4 pages, 2012.
9. ABAQUS 6.11 User Manuals, Dassault Simulia Inc., Providence, R.I., 2011.
10. C.A. Sleicher and M.W. Rouse, "A Convenient Correlation for Heat Transfer to Constant and Variable Property Fluids in Turbulent Pipe Flow," *International Journal of Heat and Mass Transfer,* Vol. 18, No. 5, 1975, pp. 677–683.
11. M.M. Langeneckert, "Influence of Mold Geometry on Heat Transfer, Thermocouple and Mold Temperatures in the Continuous Casting of Steel Slabs," M.S. thesis, University of Illinois at Urbana-Champaign, 2001.
12. L.C. Hibbeler, S. Koric, K. Xu, B.G. Thomas and C. Spangler, "Thermomechanical Modeling of Beam Blank Casting," *Iron & Steel Technology,* Vol. 6, No. 7, 2009, pp. 60–73.
13. L.C. Hibbeler, B.G. Thomas, R.C. Schimmel and G. Abbel, "Thermal Distortion of Funnel Molds," *AISTech Conference Proceedings,* Vol. I, 2011, pp. 1487–1496.
14. NIST Webbook, http://webbook.nist.gov.

Appendix

To calculate the cumulative channel area, the following equation defines the area of a semicircle of diameter d as a function of distance along the diametrical edge, for $0 \le x \le d$:

$$A(x) = \frac{d^2}{4}\left[\frac{1}{2}\arccos\left(1-2\frac{x}{d}\right)-\left(1-2\frac{x}{d}\right)\sqrt{\frac{x}{d}\left(1-\frac{x}{d}\right)}\right] \quad \text{(Eq. 29)}$$

✦

This paper was presented at AISTech 2013 — The Iron & Steel Technology Conference and Exposition, Pittsburgh, Pa., and published in the Conference Proceedings.

AIST Transactions seeks to publish original research articles focusing on scientific or technical areas relevant to the iron and steel community. All articles are peer-reviewed by Key Reviewers prior to publication.

The scope of the ***Transactions*** spans all fields of iron and steel manufacturing, from extractive metallurgy to liquid metal processing, casting, thermomechanical processing as well as coating, joining/welding and machining. Articles related to structure and properties, i.e., characterization, phase transition, chemical analysis and testing of creep, corrosion or strength are accepted. In addition, papers on process control, testing and product performance are also encouraged.

The ***Transactions*** will publish papers on basic scientific work as well as applied industrial research work. Papers discussing issues related to specific products or systems can be considered as long as the structure follows a scientific investigation/discussion, but not for the aim of advertising or for the purpose of introducing a new product. Papers should be no longer than 5,000 words, or 12 pages including figures.

Papers will either be accepted unconditionally, conditionally based on reviewers' comments, or rejected. The review process should be completed in less than two months. Upon acceptance, authors will be asked to complete a form to transfer copyright to AIST.

A PDF proof of the accepted manuscript will be sent electronically to the author(s) approximately one month prior to publication for final approval. Reprints of published manuscripts can be ordered through AIST.

Please contact me with any questions regarding ***AIST Transactions***.

Sridhar Seetharaman
AIST Transactions editor, associate professor, Carnegie Mellon Center for Iron and Steelmaking Research, Pittsburgh, Pa., USA
+1.412.268.2675,
sridhars@andrew.cmu.edu

To submit a manuscript for consideration, an electronic copy (saved as an MS-Word document) should be sent to:

AIST Transactions
Email sridhars@andrew.cmu.edu

AIST Transactions are indexed through Chemical Abstracts Service, Columbus, Ohio.

AIST Transactions Key Reviewers

Professor Chris Pistorius
Carnegie Mellon University, Pittsburgh, Pa., USA

Professor Hatem S. Zurob
McMaster University, Hamilton, Ont., Canada

Dr. P. Kaushik
senior research engineer, ArcelorMittal Global R&D Steelmaking Process Research, East Chicago, Ind., USA

Professor Patricio F. Mendez
Department of Chemical and Materials Engineering, University of Alberta, Edmonton, Alta., Canada

Professor Lifeng Zhang
School of Metallurgical and Ecological Engineering, University of Science and Technology Beijing, Beijing, China

Dr. Fred B. Fletcher
principal research engineer, ArcelorMittal Global R&D Research and Development, Coatesville, Pa., USA

Dr. Stefanie Sandlöbes
scientist, Max-Planck-Institut für Eisenforschung GmbH, Düsseldorf, Germany

Dr. Il Sohn
associate professor, Neo-Metallurgical Processing Lab, Department of Materials Science and Engineering, Yonsei University, Seoul, Korea